Computer Modeling of the Laboratory Testing of Mini-Magnetospheric Plasma Propulsion (M2P2) *†

R. M. Winglee[1], T. Ziemba[2], P. Euripides[1], and J. Slough[2]

[1]Department of Earth and Space Sciences
University of Washington
Seattle, WA 98195-1650
winglee@ess.washington.edu

[2]Department of Aeronautics and Astronautics
University of Washington
Seattle, WA 98195-2400

IEPC-01-200

Recent laboratory testing has demonstrated that the mini-magnetospheric plasma propulsion (M2P2) prototype is able to (1) efficiently produce plasma, (2) expand magnetic field lines and produce an inflated magnetosphere, and (3) deflect an external plasma source at large distances. Multi-fluid computer simulations are used to model the experimental configuration with the objective of quantifying the characteristics of the magnetic field inflation, and its deflection of an external plasma wind. The simulations show that the injection of plasma onto the closed field lines of the magnet, equatorial magnetic flux is carried out by the plasma and results in an increase in magnetic flux away from the magnet until obstructed by the chamber walls. The spatial and temporal profiles of the magnetic field perturbations derived from the simulations are shown to be consistent with the laboratory data and show the full extent of the prototype's ability to transport magnetic flux and inflate a mini-magnetosphere. Deflection of an external plasma source by the M2P2 prototype is also investigated. The simulations show that the plasma wind will be deflected by the inflated mini-magnetosphere. This deflection leads to a depletion of wind plasma in the near vicinity of the mini-magnetosphere. It is also produces a broadening and compression of the plasma plume close to the external plasma source. These very distinctive features are identified in images of the actual experiment. If the same device were deployed in space the computer modeling indicates that they could expand a mini-magnetosphere 10-20 km in radius to achieve a thrust level 1-3 N with the expenditure of only a few kW of power at less than 1 kg per day propellant consumption.

Introduction

Mini-Magnetospheric Plasma Propulsion (M2P2) [1] seeks to create a mini-magnetosphere or magnetic bubble around the spacecraft and to use the deflection of the ambient plasma to attain energy/momentum to increase the total efficiency and thrust of the system. For example, the solar wind, traveling at 400 to 800 km/s, can provide a limitless source of keV particles to provide high specific impulse propulsion. The main problem in trying to couple to the solar wind is that the solar wind has a low density (~ 6 cm^{-3}) and therefore that interaction/deflection region has to have a size of the order of a few tens of km before a thrust of a few N can be attained. The problem is akin to that of solar sails where the momentum from photons is small (albeit larger than the solar wind momentum flux) and reflecting areas of a few million m^2 are be required to provide N thrust levels. However, solar sails require the mechanical deployment of ultra thin material over large distances and the technical problems involved have yet

* Presented as Paper IEPC-01-000 at the 27th International Electric Propulsion Conference, Pasadena, CA, 15-19 October, 2001.

to be solved. The advantage of the M2P2 system is that the deployment is done by electromagnetic processes and as such does not require the deployment of any large mechanical structures.

M2P2 is able to achieve this electromagnetic deployment due to the fact that when a collisionless plasma is created in a magnetic field, that magnetic field is frozen into the plasma so that as the plasma expands the magnetic field is carried out with it. This transport of magnetic flux can be achieved with low energy plasma and the inertia of the plasma will enable it to expand a few tens of km before being swept downstream by the solar wind. Because only low energy plasma is utilized, the power requirement for the spacecraft is only a few kW [1]. The corresponding mini-magnetosphere will intercept nearly a MW of solar wind energy (some of which produces secondary heating of the plasma of the M2P2) and a thrust of a few N. With this level of thrust a small spacecraft can attain speeds of the order of 50 km/s for little more about 1 kg/day propellant consumption over an acceleration period of about 3 months.

Over the last two years, the development of an M2P2 prototype has been underway at the University of Washington. Initial results have been able to demonstrate plasma production and confinement within the desired geometry [2,3,4]. Recent experiments quantify the efficiency of the prototype and show evidence for its ability to transport magnetic flux and inflate a mini-magnetosphere [5].

In this paper, computer simulations are compared with test results of the prototype [5]. This comparison provides a full 3-D perspective of the mini-magnetosphere and provides an indication of the potential scaling of the prototype. We first briefly describe some of the details of the simulation model, and then compare the results for the prototype operating by itself. The signature for the transport of magnetic flux is very distinctive and easily identified in both the experimental data and simulations. The paper then presents results for the interaction of the mini-magnetosphere with an external plasma source and we identify key characteristics of its ability to deflect external plasma at large distances.

Numerical Model

The simulation model is essentially the same as used in the original application and configuration for the M2P2 system [1] but here the assumed configuration is designed to fully resolve processes in close proximity to the magnet. To this end, the minimum spatial resolution is set to 1 cm in the vicinity of the magnet. The magnet itself is represented by a cylinder that has a radius of 10 cm and a width of 10 cm, similar to the actual experiment. The grid spacing increases to several cm further away from the magnet.

The final size that the mini-magnetosphere can expand to is very dependent on the size of the chamber that the experiment is performed. The UW chamber where most of the detail probe data was taken has a width of 1 m. On the other hand large scale testing in the summer of 2000 [3,4] utilized the NASA Marshall Space Flight Center chamber at Test Area 300 which has a width of 6 m. A further difficulty of the modeling is that the physics of the wall interactions, which involves mirror currents, sputtering and plasma sheaths is not well incorporated in the modeling. To overcome this problem the simulation system size is assumed to be larger than the actual chamber in use and the simulations stopped before there are significant wall interactions. In the following the simulations use either a system size of 2 m for the small chamber experiments or a 16 m system for the large chamber experiments.

In the simulations the magnetic field of the magnet is represented by a point dipole. This approximation gives a ratio of 16:1 in field strength at the top of the magnet relative to the equatorial strength at the side, which is comparable to actual configuration. The field strength in all the following simulations is 1.6 kG at the top of the magnet. Superimposed on the magnet's field is the 0.32 G terrestrial field. While this field may appear small it starts to become the dominant field between 0.4 – 0.7 m from the magnet. The terrestrial field is given a slant of 10 degrees. The actual slant value is not important but we introduce it into the simulations to ensure that a non-degenerate solution is obtained. It is also important because the terrestrial field determines the position of the last closed field line attached to the magnet.

The initial conditions for the plasma density are complicated by the fact that the time step for the

simulations is inversely proportional to the maximum of the Alfvén speed, the ion velocity and the ion sound speed. In order to keep the Alfvén speed finite, a low-density background plasma is placed throughout the simulation system. In reality this background plasma is in fact often generated by low-density capacitive breakdown that occurs just prior to the initiation of the high-density helicon mode. In the following, the background plasma is assumed to have a density of 10^{11} cm^{-3} at the magnet and falls away as r^{-4}. The temperature of this background plasma is assumed to be 0.1 eV so that it has insufficient energy to make any substantial perturbations to the magnetic field. The helicon plasma at a density of 10^{13} cm^{-3} is loaded in a 3 cm diameter circle at the top and bottom of the magnet, centered 4.5 cm from the magnet wall. Its propagation into the simulation system and the corresponding field perturbations are then tracked in time and space using the plasma fluid equations [1].

Due to computational restrictions the propellant is assumed to be helium is the propellant where as in most of the actual experiments the propellant is actually argon. The reason for this is that the speed of argon is about a 1/3 slower than that of helium for the same energy and as such would require three times the computational time for the plasma to transverse the same distance. In short test runs the difference in the simulations is only the time scale so that in the following the time scale is given for helium with an outflow velocity of 18 km s^{-1}. The equivalent time scale for argon assuming an outflow of 6 km s^{-1} (which is comparable to the calculated ion speed) is added for direct comparisons with the data.

Small Chamber Inflation

In order to investigate the profile of the perturbations in the M2P2 simulations a series of pseudo-probes is placed in the equatorial plane of the simulations. The plasma density and magnetic field magnetic field at these points were continuously sampled during the simulations. The positions of these pseudo-probes overlap with positions of the Langmuir and Bdot probes used in the UW testing. Figure 1 shows a comparison between the observed field changes in the UW chamber with that derived from the 2-m computer simulations, for the case where the field outside the magnet is aligned with the terrestrial field. It is important to note that the laboratory data was achieved by repetitive shots and moving the probe. Unfortunately, there can be differences in the exact breakdown time of 50 to 200 μs. This time delay throws off some of the temporal ordering in Figure 1a but not the relative strengths of the signal. Because of the short duration of the shot, the background neutral pressure is very low at ~ 0.02 mTorr so that collisional effects are small.

The most important feature is that in both the observations and simulations, the magnetic flux is seen to be removed from the inner region of the dipole (negative perturbations) and transported to the outer regions (positive magnetic perturbations). This flux is seen to pile up such that the outer most regions see the

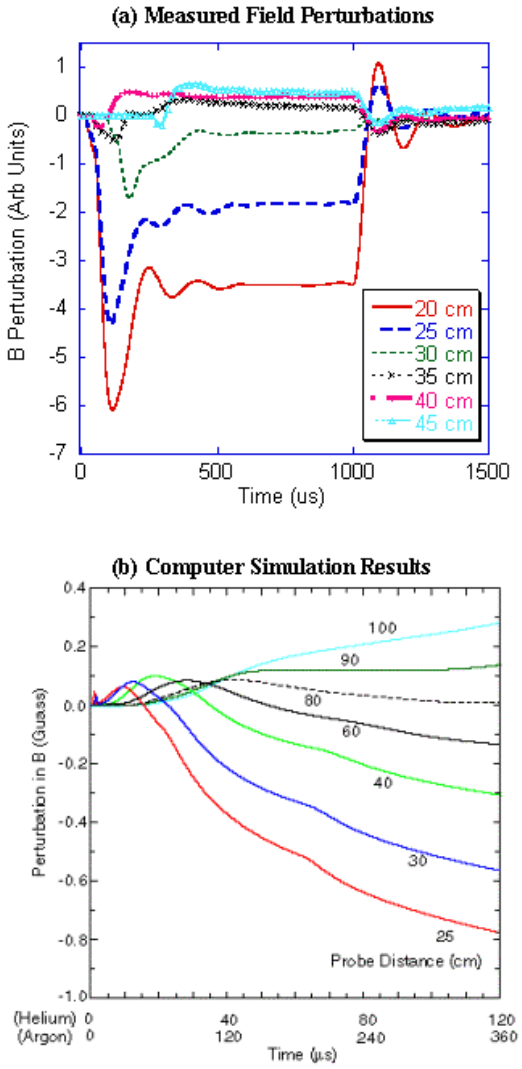

Figure 1. Comparison of (a) the observed magnetic field perturbations [5] and (b) the small chamber (2 m) simulations.

biggest increase. This signature is very distinctive in both the simulations and observations and provides strong proof that transport of magnetic flux has been achieved by the M2P2 prototype.

Another crucial feature is the rise time for the movement of magnetic flux. In both the observations and simulations the rate of charge in the magnetic field perturbations slows after only a few hundred μs. This fast rise time cannot be achieved by low energy plasma. These results suggest that the assumed speeds for the argon ions (estimated from the electron temperature measured by Langmuir probes) of 6 km/s (14 eV) argon ions is correct.

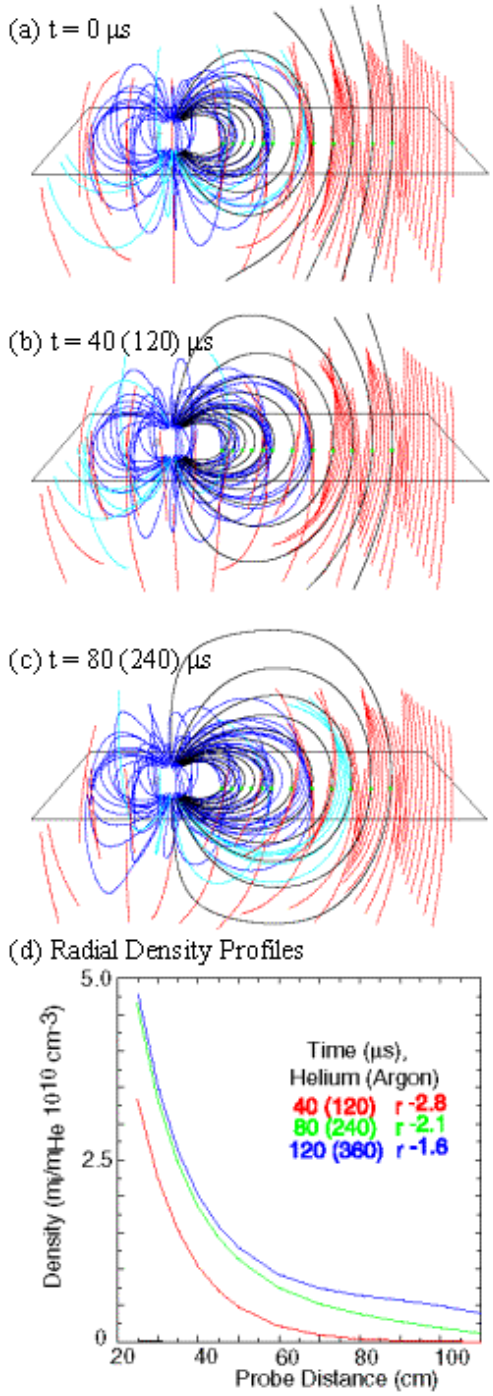

Figure 2. Mapping of the magnetic field (a)-(c) associated with the perturbations in Figure 1, and (d) the profile of the plasma density for the same period.

Note that the presence of energetic populations has been observed during operation of laboratory helicons but there the time scale has been limited to a few μs [6]. The fact that M2P2 sees a hot population over substantially longer periods may be in part due to the closed magnetic geometry of the M2P2. This geometry allows the plasma to be confined and to recirculated around the magnetic field until the latter expands into the wall. For laboratory helicons the system is linear and the magnetic field geometry is open so that wall interactions are a key in their overall equilibrium

The actual field geometry corresponding to the perturbations in Figure 1b is shown in Figure 2. The full system is shown in the figure with the magnet being 40 cm from the left hand wall and 140 cm from the right hand wall. The height and width of the system is 160 cm. The dark (light) blue lines indicated closed (open) magnetic field lines attached to the magnet. The red lines indicated terrestrial field lines that are not connected to the magnet. The green dots indicate the position of the pseudo-probes and the black lines are the field line mapping through the probe position.

Because of the terrestrial magnetic field, there are initially only closed magnetic field lines within about 70 cm of the magnet for the assumed 1.6 kG field strength at the top of the magnet. This is illustrated in the Figure 2a where the 4 outer probes (spaced 10 cm apart) are seen not to be magnetically connected to the magnet. However, with the injection of the plasma at the top and bottom of the magnet, the magnetic field is seen to expand outwards so that within 240 μs (assuming argon) even the outer most probes lie on closed field lines (Figure 2c).

Further, expansion of the field though is difficult because of the proximity of the wall. In simulations where we have assumed open boundary conditions (i.e. all plasma is lost to the walls) there is insufficient

plasma at the walls to sustain the currents required for the inflated mini-magnetosphere. For closed boundary conditions, there is a build-up of plasma pressure at the walls that impedes further expansion. However, if we utilize the larger system, the expansion is seen well beyond that indicated in Figure 2. The important point is that the a magnetic field perturbation of less than 1 G as seen in the UW experiments is all that is need to drive the field lines into the walls.

With the expansion of the mini-magnetosphere, there is a change in the density profile of the plasma within it. As shown in Figure 2d the density as it flows into the unexpanded magnetic field falls off ~ r^{-3}, i.e. n/B ~ constant. However, with the expansion of the magnetic field, the falloff rate declines to ~ r^{-2} (free expansion limit) to an overall decrease as ~ $r^{-1.5}$. This very slow fall off in density and corresponding slow fall off in magnetic field is the basic premise of the M2P2 system. With the stretching of the field lines, the field of influence of the mini-magnetosphere becomes substantially larger than with the magnet alone.

The best way to experimentally verify the predicted size of the mini-magnetosphere is through the imaging of the optical emissions of the experiment. Unfortunately the timescale of a few 100 μs is too fast for our imaging apparatus. An alternative is to run the experiment when there is a substantial number of neutrals (~ 3 mTorr) present. Under these conditions, the plasma must do work to clear the neutrals from the region (either by scattering or by ionization) otherwise losses due to recombination or diffusion lead to its depletion and inhibit the inflation of the magnetosphere. Because of the extra energy taken up in the plasma-neutral interactions, the time required for the inflation of the mini-magnetosphere is substantially increased. The field measurements of show that despite the loss inherent with plasma-neutral interactions, transport of magnetic flux still occurs similar to Figure 1 albeit at longer time scales [5].

As an example of the optical observations of inflation of a mini-magnetosphere, Figure 3 shows the images from a shot where a puff of the background neutral pressure is introduced into the system and temporally quenches the plasma. Initially the region of closed fields lines that can be seen is well inside the chamber walls and the peak emission is in fact inside the tip of the Langmuir probe. At the later times (Figures 3b and 3c), the region of closed field lines is seen to expand. Tracing of features from the bottom of the magnet for example show the emission extends both downward and further into the chamber. In addition the center of the optical emissions in the equator as well as the extreme limit of the emissions beyond the tip of the Langmuir probe are seen to move outwards. The overall shape of the optical emissions closely resembles the model results for the closed field region in Figure 2. In addition the optical emissions are seen to map into the wall of the chamber when expansion against the neutrals occurs.

Measurements of the radial density profile are shown in Figure 4 for a similar puff injection. The times shown are relative to the onset of the helicon mode. The density, like the optical emissions are peaked around the flux tube that maps to the helicon antenna. When the density is low, the fall-off beyond this peak is approximately r^{-3}, as expected from the simulations in Figure 2d and is indicative of non-inflated magnetic fields with n/B constant. However, as the density builds within the mini-magnetosphere (as seen by the rise at the peak location near 30 cm), the fall-off in density with radial distance decreases to $r^{-2.5}$ 30 ms later, and to about $r^{-1.9}$ by the end of the shot. This change in slope is similar to the simulations and indicative of the transport of magnetic field. The predicted densities are

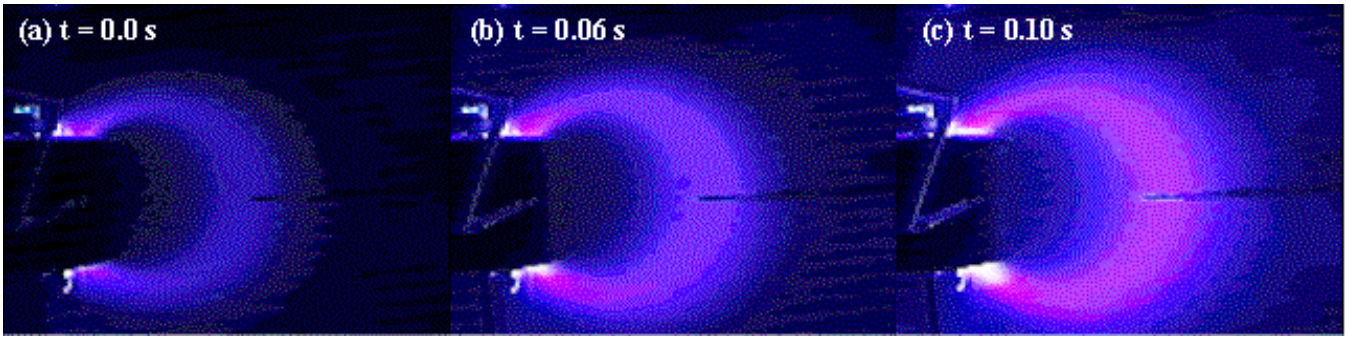

Figure 3. Optical emissions from a neutral puff during long duration testing. Time is from the introduction of the puff. The dark horizontal line of the right of each panel is a Langmuir probe. Field of view is ~40 cm.

also similar in magnitude, except that the simulations do not show the large loss of plasma at the magnet wall.

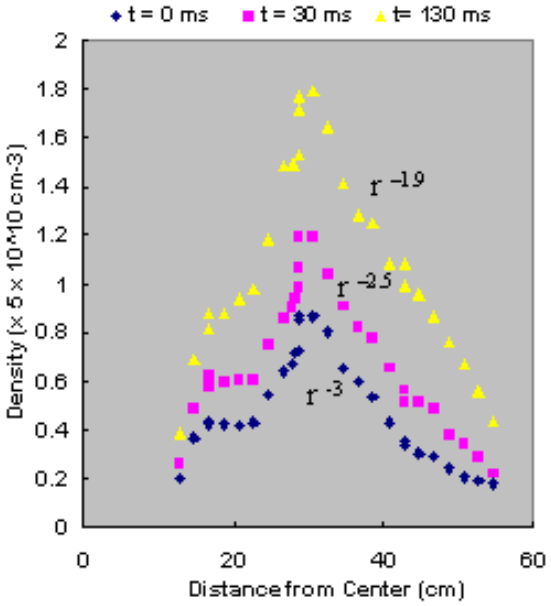

Figure 4. The radial profile of the plasma density. Time is relative to the development of the helicon mode during a neutral gas puff injection.

Large Chamber Plasma Deflection

The small chamber experiments are crucial for quantifying the plasma and magnetic field characteristics of the prototype, the transport of magnetic flux, and for calibrating the simulation model with the experimental configuration. In this section we consider the interaction of the M2P2 system with an external plasma source during large chamber experiments. The specific experiments were part of a series undertaken at the NASA Marshall Space Flight Center Test Area 300 in September 2000 [3,4]. This chamber is 32' high with a diameter of 18'. The external plasma source was provided by the Space Experiments with Particle Accelerators (SEPAC) plasma source which flew on Spacelab 1 and Altas 1.

In order to highlight the potential for long distance interaction, the simulation model utilizes the large system with a size of 16 m wide and 12.8 m high. The physical parameters for the M2P2 source are assumed the same as in the previous section, with a 3 cm diameter argon source, a density at the throat of 10^{13} cm^{-3} and an outflow velocity of 18 km/s for helium or 6 km/s for argon, embedded in a 10 cm magnet with 1.6 kG at the top of the magnet. These source characteristics are equivalent to about 9×10^{19} ions/s for argon.

The SEPAC source was approximated by an orifice of 32 cm radius (which is about twice the actual size of SEPAC). The density at the throat is assumed to be 10^{11} cm^{-3} with a speed of about 9 km/s for helium or 3 km/s for argon given a total of about 9×10^{19} ions/s for argon. Thus, the plasma flux from the two devices is well matched. The ions are also given a thermal velocity of 0.1 of their bulk velocity that leads to the thermal expansion of the SEPAC plasma. In addition the SEPAC source is pointed down by 6° similar to the experiment. This downward pointing of the source arose in the actual experiment due to warping of support strut when the device was attached to it. The distance between SEPAC and M2P2 in the model was set at 12 m as opposed to 4 m in the actual experiment to give some indication of scaling.

The SEPAC source was given the advantage in that it is operated for some time prior to the turn on the M2P2 source. This was required because the SEPAC electrodes required a warm up period for stable operation. When the M2P2 source is operated it must then pushed out the pre-existing SEPAC plasma if the magnetosphere is too expand.

Because of the large system size the simulations can only be run for a few ms. Nevertheless there are striking similarities between the experiments and simulations. For the following results, the SEPAC source is first run for 3 ms. The simulations are then continued with the M2P2 source either on or off and the difference between the two cases used to show the influence of the mini-magnetosphere.

Figure 5 shows a comparison of the density profiles for these two cases taken at time at $t = 3.6$ ms. The field of view is the full 16 m length of the simulation system. It is seen in Figure 5a that when the SEPAC source is operated by itself the plasma has time to propagate across the bulk of the simulation system but insufficient time to reach the back wall. There is some expansion of

the SEPAC plasma plume with distance due to the assumed thermal velocity of the plasma.

With the operation of the M2P2 source, there are several distinct changes in the SEPAC profile. First, there is a density minimum between the two sources and the density of the SEPAC plasma is actually lower in the middle region than when SEPAC operates by itself. The second effect is that the plasma plume is substantially thickened both horizontally as well as vertically. Third and most surprisingly is that the plasma plume is affected all the way in to close proximity of the plasma source. For example the regions of density at 10^{10} cm^{-3} retreat from the middle of the system in Figure 5a to near the SEPAC source in Figure 5b.

This deflection of the external plasma is associated with the inflation of the mini-magnetosphere as seen in Figure 6. The field of view is decreased to 7 m so that the interaction region can be more easily seen. In Figure 6a, without the operation of the M2P2 source the magnetic field is dominated by the terrestrial field and the field from the magnet only has a significant influence out to about 0.7 m. As a result, the dipole field on this scale appears essentially negligible. The operation of the SEPAC source produces a weak bending of the field lines on the right hand side of the field of view. Its penetration into the field of view is also seen in the pressure contours shown in the bottom of the panels.

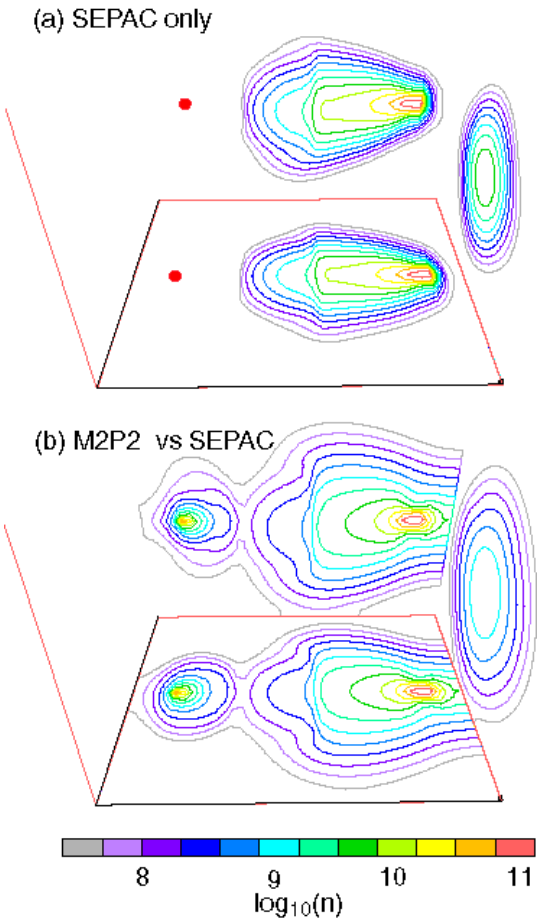

Figure 5. Density contours in cm^{-3} during (a) operation of the SEPAC source from 0-3.6 ms and (b) operation of the SEPAC source through t = 3.6 ms with the M2P2 source on from 3.0 to 3.6 ms. The bottom contours of each panel show an equatorial cut through the center, the back contours a vertical cut through the center, and the right contours a cross-section through the model of the simulation box. The red dots in (a) show the position of the M2P2 source.

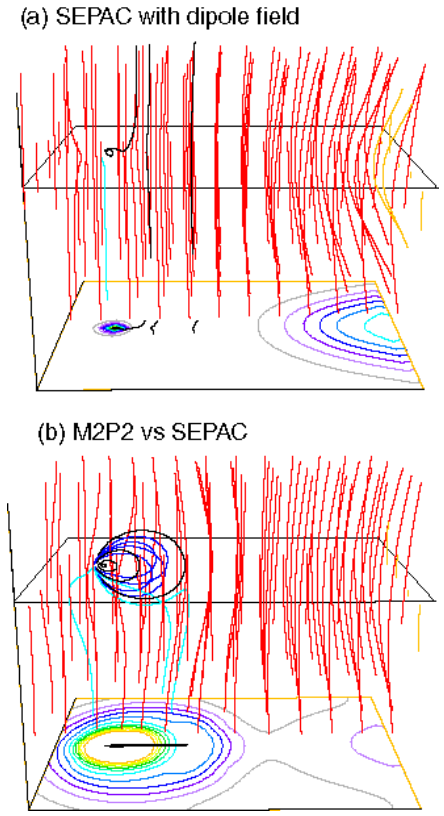

Figure 6. Magnetic field mapping corresponding to Figure 5. The format is the same as Figure 2 except the field of view is 7 m and the contours of the equatorial plasma pressure added at the bottom.

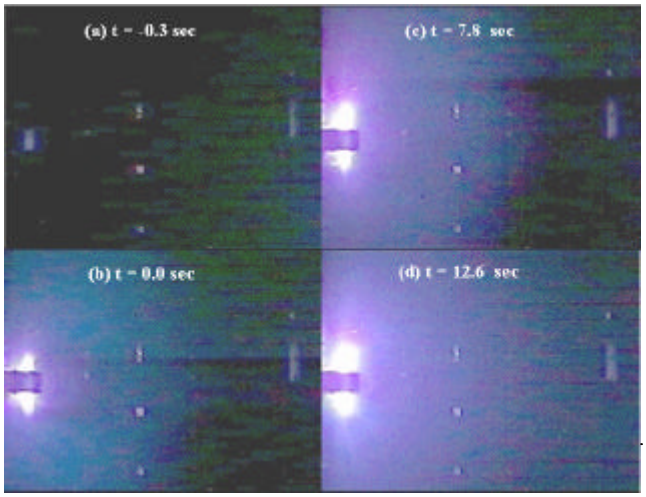

Figure 7. Images at fixed gain of the operation of the M2P2 source (left hand side) as it pushes against the SEPAC source (to the right). The field of view is 2m.

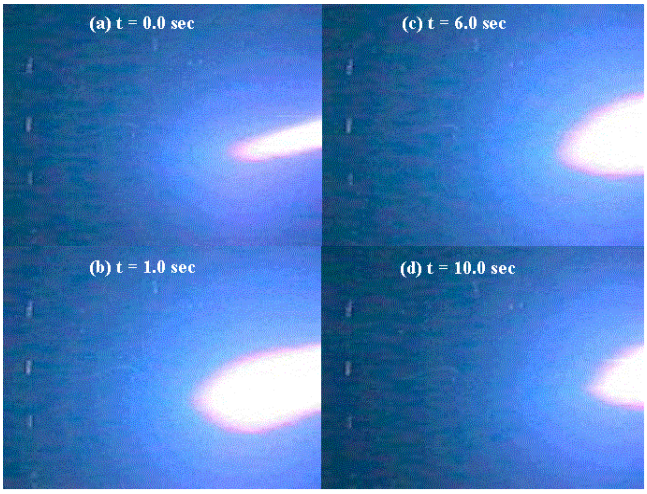

Figure 8. Images of the SEPAC source covering the same period and scale size as Figure 7.

With the operation of the M2P2 source (Figure 6b) the magnetic field is seen to expand several times its initial size, or several tens of magnet radii. The mini-magnetosphere appears to still be growing but due to computational restrictions we have not been able to follow the evolution further at this time. One of the consequences of the inflation of the mini-magnetosphere is that it reverses the concavity of the terrestrial field lines produced by the operation of the SEPAC source. This change in concavity is associated with a net flow of plasma to the right that leads to a decrease in the presence of SEPAC plasma in the field of view. This effect is seen as a reduction in the pressure contours on the right hand side of Figure 6b.

Several of these simulation features were seen in the MSFC Test Area 300 experiments. These features include the plasma depletion layer between the two plasmas, the expulsion of the SEPAC plasma from the region between the two plasmas, and the broadening of the plasma jet close to the SEPAC source. These processes for example can be seen through images taken from two pc cameras. The two cameras were required because the 4 m separation between M2P2 and SEPAC could not be caught in a single camera.

Figure 7 shows images from the pc camera that was pointed towards the M2P2 source. As noted earlier, SEPAC is turned on before the M2P2 and its penetration into the field of view can be seen by the faint emissions on the right hand side of Figure 7a.

When M2P2 is turned on (Figure 7b) the emissions on the right hand side from SEPAC are seen to decline, indicating a reduction in the electron population from SEPAC in the region, similar to the simulations in Figure 5. Further, a minimum in the optical emissions is seen between M2P2 and SEPAC. This feature is appears relatively stable as it is seen throughout the experiment (Figures 7b-c).

This gap is analogous to the magnetopause of the earth where there is deflection of solar wind by the terrestrial magnetosphere. Its persistence in the experiment indicates that the mini-magnetosphere is stable over long periods. Furthermore the magnetopause is seen to move to the right as the operation of the M2P2 continues, moving almost out field of view in Figure 7d. This motion provides further support that the plasma in the mini-magnetosphere is well confined and that the continued plasma production leads to the increasing build up of the mini-magnetosphere.

The effect of the plasma deflection on the SEPAC source is further illustrated in Figure 8 which shows images from the second pc camera viewing the SEPAC source. It is seen that initially the plasma plume from SEPAC is very narrow (Figure 8a). At turn on of the M2P2 there is an enhancement in the SEPAC emissions that appears as a broadening and expansion of the plume and an increase in the brightness on the left hand side of the image. We attribute this additional emission to an increase in the efficiency in plasma production at

SEPAC due to the presence of additional electrons from M2P2. However, as the operation of both sources continues, the emissions on the left hand side are seen to diminish in association with the expansion of the mini-magnetosphere seen in Figure 7. The most intense part of the plasma plume remains broadened but its length is substantially shortened. This situation is similar to the simulation results of Figure 5.

In conjunction with the shrinking of the plasma plume, there is also a reduction in the intensity of the emissions on the left hand in conjunction with the expansion of the mini-magnetosphere. These effects are being seen at distances a few tens of magnetic radii from M2P2 and demonstrate the large range of influence that magnetized plasmas can have when generated in closed field geometries.

Conclusion

In this paper signatures for the expansion of a mini-magnetosphere have been explored through comparative results between numerical simulations and laboratory results. It has been shown that the transport of flux within the mini-magnetosphere has a very distinctive signature, where the flux inside the magnetosphere is seen to decline and the flux outside the initial closed region of the vacuum dipole is seen to increase. As flux is transported outwards, both the simulations and observations show a pile up of the terrestrial magnetic field.

The perturbations observed to date might be considered small at only ~ 1 G, but this change in magnetic field is sufficient to drive the field lines into the walls for the laboratory chambers that are available. In addition, both the simulations and experimental results show that this same type of magnetic field perturbation is able to deflect plasma at large distances, and produces observable effects all the way into the throat of an external plasma source.

These results are all strong indicators that the inflation of a mini-magnetosphere can be achieved with existing technology. The closed magnetic field geometry of M2P2 provides an efficient means for deflection external plasma winds at very much larger distances than can be accomplished by a magnet alone.

The inflation and deflection are the key tenements of the M2P2 system and the confirmation of the simulations results with the laboratory results provide strong evidence that the high thrust levels (1-3 N) reported in the original description [1] should be achievable for low energy input (~ kW) and low propellant consumption (< 1 kg/day). Further testing to measure the thrust levels attainable by the prototype still have to be made. But the above results suggest that the relevant question is not whether the device can attain additional thrust from the deflection of an external plasma, but what is its actual efficiency.

Acknowledgements
This work was supported by NASA's Institute for Advance Concepts grant 07600-032, and NASA MSFC grant NAG8-1801 to the Univ. of Washington. The simulations were supported by the Cray T-90 at the San Diego Supercomputing Center which is supported by NSF.

References

[1] R. M. Winglee, J. Slough, T. Ziemba, and A. Goodson, "Mini-magnetospheric plasma propulsion: Tapping the energy of the solar wind for spacecraft propulsion," *2000, J. Geophys. Res.*, ***105***, *20,833*.

[2] R. M. Winglee, J. Slough, T. Ziemba, and A. Goodson, "Mini-Magnetospheric Plasma Propulsion: High Speed Propulsion Sailing the Solar Wind," *2000, Space Technology and Applications International Forum-2000*, edited by M. S. El-Genk, *American Institute of Physics*, ***CP504***, *p. 962.*

[3] R. M. Winglee, T. Ziemba, J. Slough, P. Euripides and D. Gallagher, "Laboratory testing of mini-magnetospheric plasma propulsion prototype," , *2001 Space Technology and Applications International Forum-2001*, edited by M. S. El-Genk, *American Institute of Physics*, ***CP552***, *p. 407.*

[4] R. M. Winglee, T. Ziemba, J. Slough, P. Euripides, D. Gallagher, P. Craven, W. Tomlinson, J. Cravens and J. Burch, "Large Scale Laboratory Testing of Mini-Magnetospheric Plasma Propulsion (M2P2) – Enabling Technology for Planetary Exploration," 2001, *12th Annual Advanced Space Propulsion Workshop Proc.*, April 3 - 5, 2001.

[5] T. Ziemba, R. M. Winglee, R. M. Winglee, and P. Euripides, "Parameterization of the Laboratory

Performance of the Mini-Magnetospheric Plasma Propulsion (M2P2) Prototype," *2001, 27th International Electric Propulsion Conference*, 15-19 October, 2001, this issue.

[6] Boswell, R. W., and D. Vender, "An experimental study of breakdown in a pulsed helicon plasma," 1995, *Plasma Sources, Sci. and Tech., **4,** 534.*